Supplementary Materials

A biocompatible integrated bladder electronics for wireless capacity monitoring assessment

Lin Duan, Ming-Liang Jin*

School of Automation, Qingdao University, Qingdao 266071, Shandong, China.

***Correspondence to:** Prof. Ming-Liang Jin, School of Automation, Qingdao University, Ningxia Road, Qingdao 266071, Shandong, China. E-mail: jinmingliang@qdu.edu.cn

MAIN TEXT

Fabrication of conductive film for chitosan-acetic acid electrode patch

The raw materials employed in the fabrication of the patch electrode substrate are chitosan powder and an acetic acid solution.[1,2] The fabrication process is outlined below: 3 g of chitosan powder is mixed with 90 ml of acetic acid solution, and then glycerol with different volume ratios (0, 2%, 4%, 6%, 8%) is added to configure a certain amount of chitosan solution. Subsequently, the mixed solution was stirred with a magnetic stirrer at a temperature of 60°C until the chitosan powder was completely dissolved, at which time the chitosan solution was yellowish and viscous. It was then stirred again at high speed for 10 minutes and left to stand for two hours until the air bubbles disappeared completely. The solution casting method was employed to ensure uniform distribution of the chitosan solution on a disc-shaped vessel. and it was placed into a hot blast drying oven for 20 min and then taken out, with the temperature set at 40 °C, and naturally cooled in a room temperature environment. This process resulted in the formation of a flexible film. The chitosan film was immersed in a 0.1 mol sodium hydroxide standard solution for the purpose of acid-base neutralization. Thereafter, the chitosan film was gently peeled off in order to obtain the chitosan-acetate gel, which was then washed with deionized water and subsequently wrapped in a sealing film for storage.

Integration of electronics hardware system design

According to the overall architecture of the system function and hardware composition requirements after the design of the schematic diagram, it will be imported into the printed circuit board design software, the use of the design software Altium designer.[3-5] In accordance with the electrical properties of the circuit board for the layering partition, mechanical layer set the size of the main control board and other mechanical information, signal layer to place the components, wiring and soldering, component layer for resistive soldering and silk screen printing. Layout of signal, ground and power lines in the inner layer to ensure compliance with impedance control specifications, appropriate adjustment of component location, complete the printed circuit board layout, and final process ends with the completion of the printed circuit board.

Equivalent model calculations for bioelectrical impedance of individual cells in bladder tissue Eq.

Here, C_{cm} represents the cell membrane capacitance of the bladder cell, R_{if} denotes the intracellular fluid resistance of the bladder cell, and R_{ef} denotes the extracellular fluid resistance of the bladder cell. The impedance is comprised of a real and an imaginary part, with the real part indicating conductivity and the imaginary part indicating capacitance.

Consequently, the bladder impedance, Z_b, can be expressed as

$$Z_b = R_{ef} + \frac{X_{C_{cm}} R_{if}}{X_{C_{cm}} + jR_{if}} = \frac{R_{ef}\left(1+R_{if}{}^2\omega^2 C_{cm}{}^2\right)+R_{if}}{1+R_{if}{}^2\omega^2 C_{cm}{}^2} - j\frac{R_{if}{}^2\omega C_{cm}}{1+R_{if}{}^2\omega^2 C_{cm}{}^2} \tag{1}$$

In the aforementioned equation, ω represents the angular frequency, while $X_{C_{cm}}$ denotes the capacitive resistance of the cytosolic membrane capacitance C_{cm} of the bladder cell. Both of these variables are subject to the following equation:

$$X_{C_{cm}} = \frac{1}{\omega C_{cm}} \tag{2}$$

$$\omega = 2\pi f \tag{3}$$

The results of the calculations indicate that the mode of the bladder impedance Z_b, and its phase alias are as follows:

$$|Z_b| = \sqrt{\frac{\left[R_{ef}\left(1+R_{if}{}^2\omega^2 C_{cm}{}^2\right)+R_{if}\right]^2 + R_{if}{}^4\omega^2 C_{cm}{}^2}{\left(1+R_{if}{}^2\omega^2 C_{cm}{}^2\right)^2}} \tag{4}$$

$$\theta_{Z_b} = -\tan^{-1}\left[\frac{R_{if}{}^2\omega C_{cm}}{1+R_{if}{}^2\omega^2 C_{cm}{}^2} \Bigg/ \frac{R_{ef}\left(1+R_{if}{}^2\omega^2 C_{cm}{}^2\right)+R_{if}}{1+R_{if}{}^2\omega^2 C_{cm}{}^2}\right] \tag{5}$$

Supplementary Table 1. Comparison of the size of traditional equipment and development equipment

Device Name	Type	Dimensions (L × W)	Reference
Z3 Bladder Scanner	Ultrasound Bladder Scanner	Approx. 30 cm × 20 cm	-
Vitascan cVue	Ultrasound Bladder Scanner	25 cm × 20 cm	-
Urinary Catheter	Urinary Drainage Device	Catheter length approx. 40 cm	[6]
Magnetic Resonance Imaging (MRI)	High-Resolution Imaging Device	Approx. 2.5 m × 2.5 m	[7-9]
Computed Tomography (CT)	High-Resolution Imaging Device	Approx. 2.0 m × 1.0 m	[8,9]
Our Developed Device	Bioelectrical Impedance Analysis Device	16 cm × 8 cm	This work

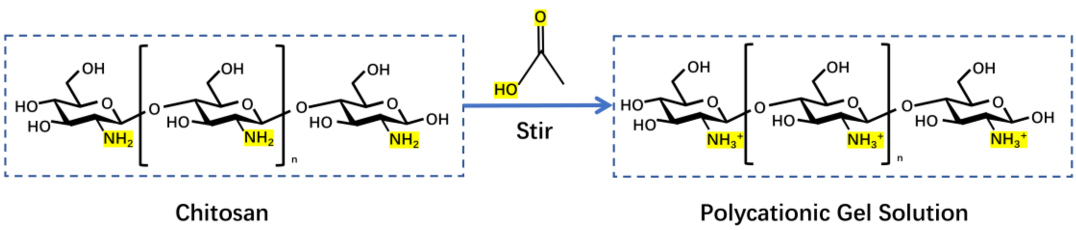

Supplementary Figure 1. The chemical assembly scheme of chitosan and acetic acid in biocompatible flexible electrode patches.

(1) In an aqueous solution, the acetic acid molecule undergoes protonation, resulting in the dissociation of carboxyl ions and hydrogen ions.

$$CH_3COOH \rightarrow CH_3COO^- + H^+ \tag{6}$$

(2) The amino groups present in chitosan molecules undergo a process of protonation, resulting in the formation of ammonium ions (NH_3^+). This transformation enables the generation of polycationic gel solutions.[10-12]

$$—NH_2 + H^+ \rightarrow —NH_3^+ \tag{7}$$

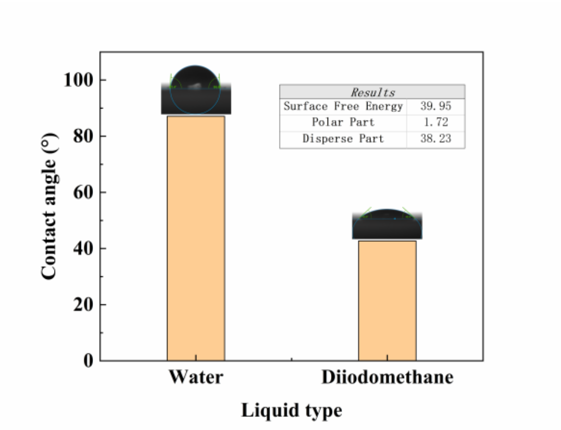

A

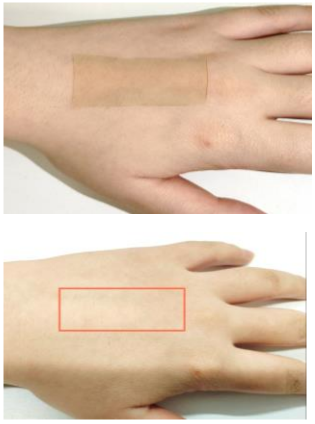

B

Supplementary Figure 2. The assessment of thin film biocompatibility. **(**A) Surface energy test. The contact angle of water on the film was found to be 87.1°, while that of diiodomethane was 42.7°. The surface energy of the chitosan film is 39.95 mJ/m²; (B) Skin irritation test. The patch was applied to the skin for 24 h (top), and upon removal, there was no redness or itching (bottom).

A

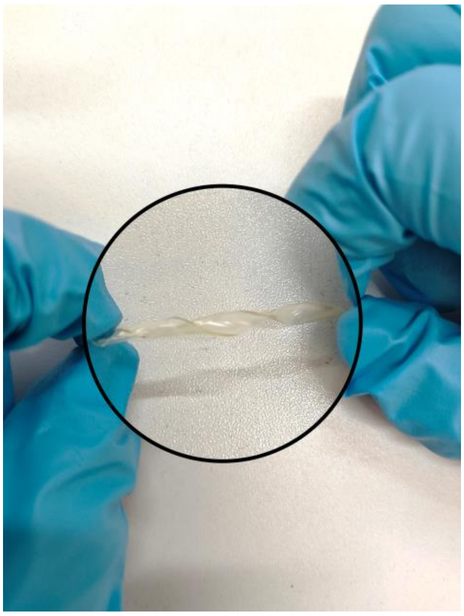

B

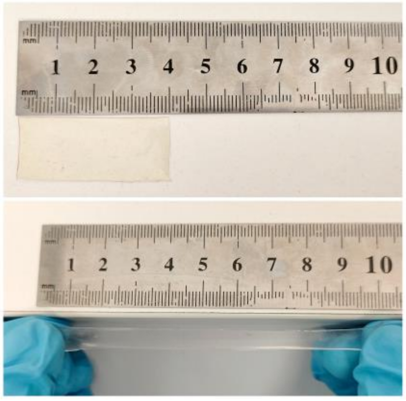

C

Supplementary Figure 3. A demonstration of the functionality of biocompatible chitosan-acetate conductive films. Excellent properties of electrically conductive films, including (A) adhesion; (B) mechanical flexibility; and (C) elongation, with a film length of 4 cm before stretching and 10 cm after stretching, with an elongation of 150 per cent.

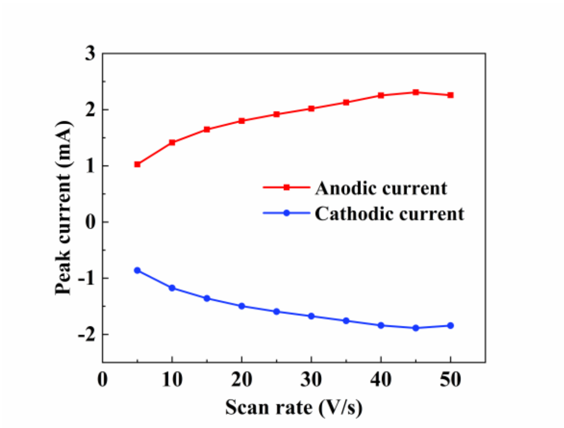

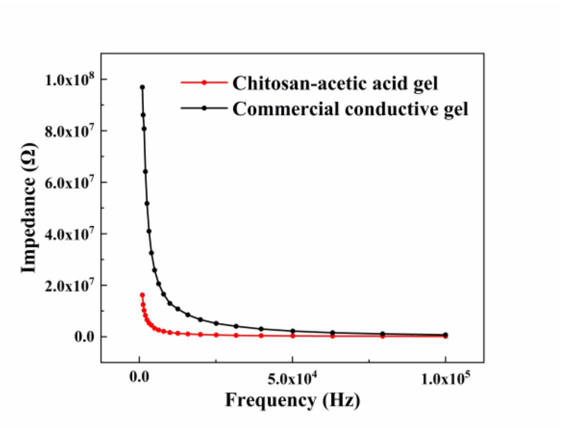

A **B**

Supplementary Figure 4. Performance studies of biocompatible electrode patch. (A) Peak voltammetry characteristics of electrode patches at different rates (5-50mV/s); (B) A comparative analysis of the electrical conductivity of commercially available conductive gel electrode patches with chitosan-acetate gel electrode patches at varying frequencies.

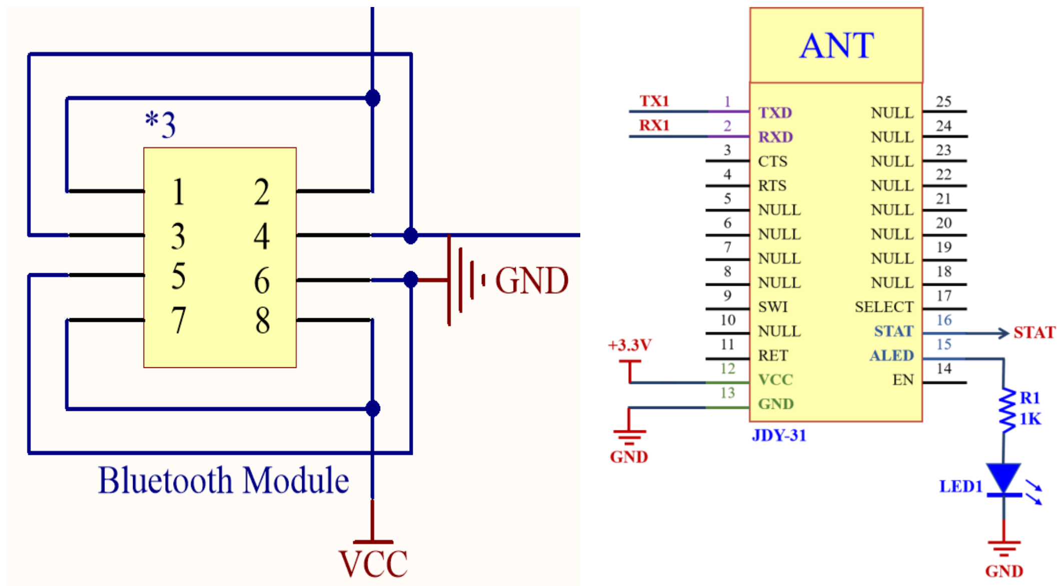

A B

Supplementary Figure 5. The system Bluetooth module (A) circuit schematic and (B) pinout diagram. The Bluetooth module facilitates data transfer and real-time monitoring between the electronic device and the mobile phone.

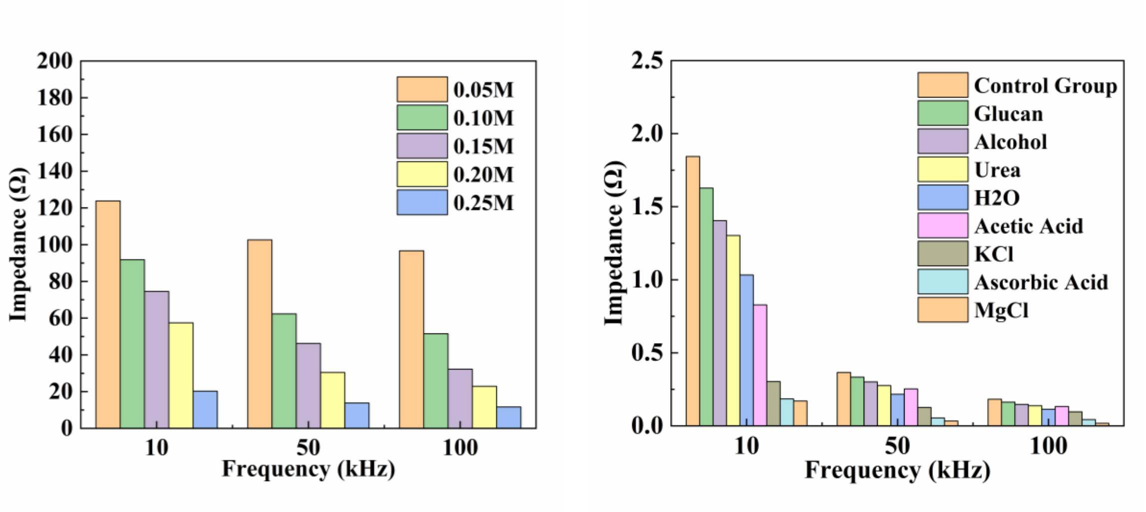

A B

Supplementary Figure 6. The impedance response of the electronic system. (A) different concentrations of NaCl solutions and (B) H_2O, urea, glucan, acetic acid, alcohol, potassium chloride, ascorbic acid, and magnesium chloride solutions at three different frequencies, 10 kHz, 50 kHz, and 100 kHz.

Supplementary Table 2. Discussion of material stability for long-term use in device development

Equipment Components	Material Used	Material Stability in Long-term Use	Reference
Printed Circuit Board (PCB)	Epoxy resin, fiberglass	High chemical resistance, stable dielectric properties, moderate wear resistance	[13]
Encapsulation Shell	Polyurethane (PU)	Excellent flexibility and chemical stability, resistant to environmental stress	[14]
Electrode Patches	Chitosan, acetic acid, glycerol	Stable impedance with RSD of 0.791% over 10 days	[15]
Connecting Leads	conductive polymers	High conductivity retention, corrosion-resistant coating ensures stability	[16]
Battery Housing	Polycarbonate (PC)	High impact resistance, stable under temperature fluctuations	[17]

REFERENCES

1. Qian J, Wang X, Chen Y, et al. The correlation of molecule weight of chitosan oligomers with the corresponding viscosity and antibacterial activity. *Carbohydrate Research.* 2023;530. doi: 10.1016/j.carres.2023.108860
2. Du Y, Kim JH, Kong H, et al. Biocompatible Electronic Skins for Cardiovascular Health Monitoring. *Advanced Healthcare Materials.* 2024;13(16). doi: 10.1002/adhm.202303461
3. Shamkhalichenar H, Bueche CJ, Choi J-W. Printed circuit board (PCB) technology for electrochemical sensors and sensing platforms. *Biosensors.* 2020;10(11):159. doi: 10.3390/bios10110159
4. Malinowski A, Yu H. Comparison of embedded system design for industrial applications. *IEEE transactions on industrial informatics.* 2011;7(2):244-254. doi: 10.1109/tii.2011.2124466
5. Waffenschmidt E, Ackermann B, Ferreira JA. Design method and material technologies for passives in printed circuit board embedded circuits. *IEEE*

Transactions on Power Electronics. 2005;20(3):576-584. doi: 10.1109/tpel.2005.846530
6. Domingues B, Pacheco M, de la Cruz JE, et al. Future directions for ureteral stent technology: from bench to the market. *Advanced Therapeutics.* 2022;5(1):2100158. doi: 10.1002/adtp.202100158
7. Caglic I, Panebianco V, Vargas HA, et al. MRI of bladder cancer: local and nodal staging. *Journal of Magnetic Resonance Imaging.* 2020;52(3):649-667. doi: 10.1002/jmri.27090
8. Bandyk MG, Gopireddy DR, Lall C, et al. MRI and CT bladder segmentation from classical to deep learning based approaches: Current limitations and lessons. *Computers in Biology and Medicine.* 2021;134:104472. doi: 10.1016/j.compbiomed.2021.104472
9. El-Ghar MA, Farg H, Sharaf DE, et al. CT and MRI in urinary tract infections: a spectrum of different imaging findings. *Medicina.* 2021;57(1):32. doi: 10.3390/medicina57010032
10. Bodnar M, Hartmann JF, Borbely J. Preparation and Characterization of Chitosan-Based Nanoparticles. *Biomacromolecules.* 2005/09/01 2005;6(5):2521-2527. doi: 10.1021/bm0502258
11. Shariatinia Z, Jalali AM. Chitosan-based hydrogels: Preparation, properties and applications. *International Journal of Biological Macromolecules.* 2018;115:194-220. doi: 10.1016/j.ijbiomac.2018.04.034
12. Qiao C, Ma X, Wang X, et al. Structure and properties of chitosan films: Effect of the type of solvent acid. *Lwt.* 2021;135. doi: 10.1016/j.lwt.2020.109984
13. Perdigones F, Quero JM. Printed circuit boards: The layers' functions for electronic and biomedical engineering. *Micromachines.* 2022;13(3):460. doi: 10.3390/mi13030460
14. Sikdar P, Dip TM, Dhar AK, et al. Polyurethane (PU) based multifunctional materials: Emerging paradigm for functional textiles, smart, and biomedical applications. *Journal of Applied Polymer Science.* 2022;139(38):e52832. doi: 10.1002/app.52832
15. Sheth P, Patil D, Kandasubramanian B, et al. Advancements in chitosan membranes for promising secondary batteries. *Polymer Bulletin.* 2024;81(17):15319-15348. doi: 10.1007/s00289-024-05448-x
16. Yang J, Dong H, Huang Z, et al. Exploration of organic matrixes in conductive

silver paste: a comprehensive review. *Journal of Materials Science: Materials in Electronics.* 2024;35(18):1248. doi: 10.1007/s10854-024-13047-9

17. Gohil M, Joshi G. Perspective of polycarbonate composites and blends properties, applications, and future development: A review. *Green Sustainable Process for Chemical and Environmental Engineering and Science.* 2022:393-424. doi: 10.1016/b978-0-323-99643-3.00012-7